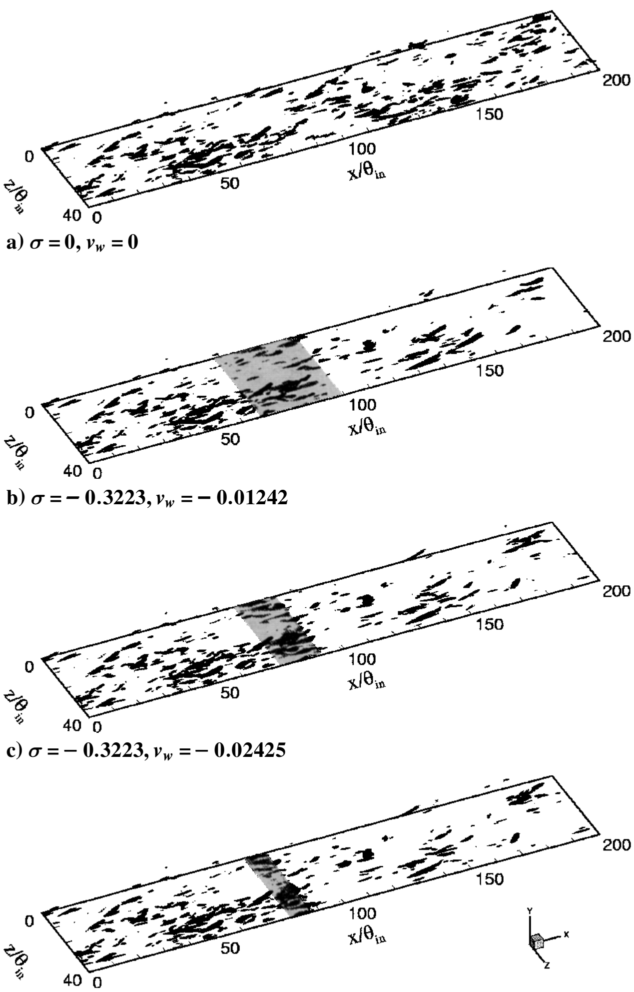

a) $\sigma = 0, v_w = 0$

b) $\sigma = -0.3223, v_w = -0.01242$

c) $\sigma = -0.3223, v_w = -0.02425$

d) $\sigma = -0.3223, v_w = -0.04630$

Fig. 6 Three-dimensional views of the streamwise vortices very near the wall for suction (isosurfaces of $|\omega_x| = 0.35U_\infty/\theta_{in}$): a) no suction, b) $v_w/U_\infty = -0.01242$, c) $v_w/U_\infty = -0.02425$, and d) $v_w/U_\infty = -0.04630$.

Three-dimensional views of the streamwise vortices very near the wall are illustrated in Figs. 5 and 6. These instantaneous flow visualizations are helpful in capturing the global effect of v_w on the flow. The contour values of ω_x are $|\omega_x| = 0.35U_\infty/\theta_{in}$. The regions of blowing/suction are denoted in gray. For blowing (Fig. 5) the vortical structures are lifted up above the slot and become much stronger downstream.[4] An interesting finding is that the strengthened near-wall vortices are accumulated at $x/\theta_{in} \simeq 107$, regardless of v_w. The maximum $\Delta\omega'_{x,\mathrm{rms}} (= \sqrt{\omega'^2_x} - \sqrt{\omega'^2_{x,0}})$ is located at $(x/\theta_{in}, y^+_{in}) \simeq (107, 15)$ for three blowing cases. For suction (Fig. 6), however, the vortical structures are drawn toward the wall above the slot and become weaker downstream.[4] Because of the suction, the near-wall vortices are substantially weakened at the immediate rear of the slot. Just after the suction, they begin to recover without relaxation. This reflects that $\int(\partial P/\partial x)\,\mathrm{d}y$ and $\Delta p'_{w,\mathrm{rms}}$ recover monotonously for suction as shown in Figs. 3b and 4b.

Conclusions

The role of v_w at a fixed value of σ is tested for blowing/suction. Toward this end, a direct numerical simulation of turbulent boundary layer is performed at $Re_\theta = 300$. The results for three different values of v_w at a constant $|\sigma| = 0.322$ reveal that $|\Delta p'_{w,\mathrm{rms}}|$ and $|\int(\partial P/\partial x)\,\mathrm{d}y|$ increase with increasing $|v_w|$ above the slot. A local maximum exists after the slot for blowing. The local maxima for three blowing cases are located at the same position ($x/\theta_{in} \simeq 104$). The streamwise variation of $c_f/2$ for blowing is much smaller than for suction. For blowing the strengthened near-wall vortices are accumulated at $x/\theta_{in} \simeq 107$, regardless of v_w. For suction, however, the near-wall vortices are weakened at the immediate rear of the slot.

Acknowledgment

This research was supported by a grant from the National Research Laboratory of the Ministry of Science and Technology, Republic of Korea.

References

[1] Antonia, R. A., Zhu, Y., and Sokolov, M., "Effect of Concentrated Wall Suction on a Turbulent Boundary Layer," *Physics of Fluids*, Vol. 7, No. 10, 1995, pp. 2465–2474.

[2] Krogstad, P. Å., and Kourakine, A., "Some Effects of Localized Injection on the Turbulence Structure in a Boundary Layer," *Physics of Fluids*, Vol. 12, No. 11, 2000, pp. 2990–2999.

[3] Chung, Y. M., and Sung, H. J., "Initial Relaxation of Spatially Evolving Turbulent Channel Flow with Blowing and Suction," *AIAA Journal*, Vol. 39, No. 11, 2001, pp. 2091–2099.

[4] Park, J., and Choi, H., "Effects of Uniform Blowing or Suction from a Spanwise Slot on a Turbulent Boundary Layer Flow," *Physics of Fluids*, Vol. 11, No. 10, 1999, pp. 3095–3105.

[5] Sano, M., and Hirayama, N., "Turbulent Boundary Layers with Injection and Suction Through a Slit. First Report: Mean and Turbulence Characteristics," *Bulletin of the Japan Society of Mechanical Engineering*, Vol. 28, No. 239, 1985, pp. 807–814.

[6] Lund, T. S., Wu, X., and Squires, K. D., "Generation of Turbulent Inflow Data for Spatially-Developing Boundary Layer Simulation," *Journal of Computational Physics*, Vol. 140, 1998, pp. 233–258.

[7] Kim, K., Baek, S.-J., and Sung, H. J., "An Implicit Velocity Decoupling Procedure for the Incompressible Navier–Stokes Equations," *International Journal for Numerical Method in Fluids* (to be published).

P. R. Bandyopadhyay
Associate Editor

Surface-Shear-Stress Pulses in Adverse-Pressure-Gradient Turbulent Boundary Layers

V. A. Sandborn*
Colorado State University,
Fort Collins, Colorado 80523-1320

I. Introduction

LARGE-MAGNITUDE surface-shear-stress pulses, which are present in all turbulent boundary layers, do not appear to be accounted for in current turbulence models. The pulses are related to the "sweep" motions observed near the surface in shear flows. These pulses are not only large in amplitude, but also the highest frequencies present. Thus, low-frequency (large-eddy) simulation models might not be able to capture them.[1]

Surface hot-wire evaluations of the time-dependent surface shear stress were employed to identify characteristic magnitudes and times for the pulses.

II. Experimental Results

Figure 1 shows a typical time trace of the surface shear stress obtained in an adverse-pressure-gradent turbulent boundary layer. The trace was for flow along a curved floor in a 61 × 61-cm wind tunnel (see Ref. 2 for experimental setup). Figure 2 shows the pressure-gradient variations along the curved floor for a number of Reynolds numbers (q is the upstream dynamic pressure). "Intermittent" turbulent separation occurred near the end of the curved

Received 9 September 2000; revision received 14 July 2001; accepted for publication 14 September 2001.

*Emeritus Professor, Civil Engineering. Senior Member AIAA.

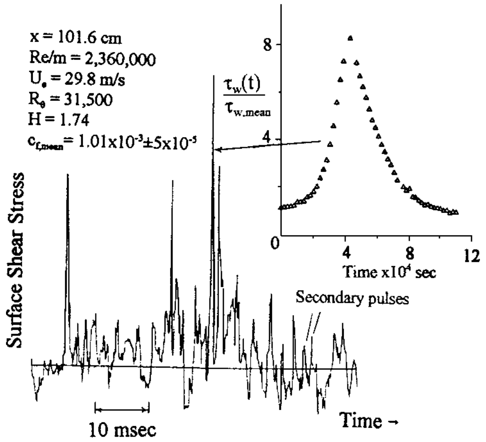

Fig. 1 Surface hot-wire time trace.

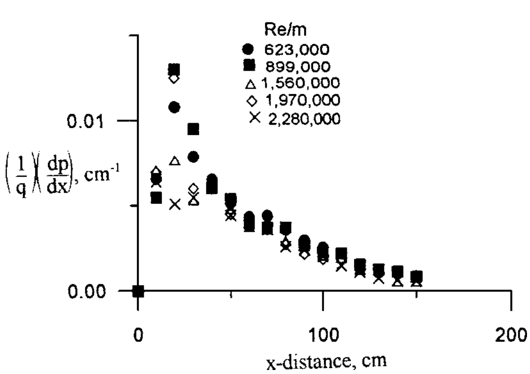

Fig. 2 Pressure-gradient variation along the curved floor.

section ($x = 150$ cm, where velocity profile form factor $H = 2.55$–2.65 and the ratio of displacement to boundary thickness is equal 0.36 to 0.375).[3] As seen on Fig. 1, large-magnitude, high-frequency pulses of surface shear stress occur at random times. The occurrence of the pulses was shown to be related to coherent event timescales present in turbulent boundary layers.[4] Because the coherent events are three-dimensional, the pulses observed vary both in magnitude and shape.

An expanded timescale for a large pulse is shown on the insert of Fig. 1: the relative values are accurate to $\pm.01$. The pulse shown exceeds the mean shear by greater than eight times. The rise time of the pulses depended on the flow velocity. For the pulse shown, a rise time of approximately 2×10^{-4} s is indicated. (The surface hot-wire-anemometer rise time, determined with a pulse tube, was measured as 5×10^{-5} s.) At lower flow velocities rise times of the order of milliseconds are observed. For the present study the surface hot-wire outputs were quasi-linearized using a commercial power law (5.2 power) linearizer. A two-dimensional, fully developed, channel flow device was employed to calibrate the sensors directly while mounted in the surface.

Estimates of the maximum pulse magnitudes were determined employing a hybrid probability computer, with sampling times of 80–100 s at rates of 5000 samples per second. The sample rate was marginal for the higher flow velocities; thus, the indicated maximums could be lower than the actual peaks. Figure 3 shows the maximum pulse values as a function of Reynolds number and distance along the surface. At each location the pulse maximum surface shear stress was found to increase as the Reynolds number increased; however, the mean shear $\tau_{w,\text{ref}}$ at $x = 15.2$ cm increased more rapidly. Near intermittent separation the maximum values vary directly as the reference shear and are nearly two times the upstream mean values. These large pulses appear to produce intermittent separation.[3]

Estimates of the minimum values of the surface shear stress were obtained directly from the digital oscilloscope traces, such as shown on Fig. 1. Figure 4 shows minimum values of the skin-friction coefficient obtained at two locations in the adverse-pressure-gradient flow. As the minimum shear approaches zero, the noise level of the anemometer-linearizer system limits the accuracy. The uncertainty of $c_{f,\min}$ was of the order of $\pm 2 \times 10^{-4}$. The absolute value of the minimum shear stress, at both x locations, becomes progressively smaller as the Reynolds number decreased; thus, the present data were limited to momentum thickness Reynolds numbers R_θ greater than 1×10^4. For reference, measurements of $c_{f,\min}$ in a zero-pressure-gradient flow[4] are also included on Fig. 4. Direct correspondence with momentum thickness Reynolds number between zero and adverse-pressure-gradient flows would not be expected.

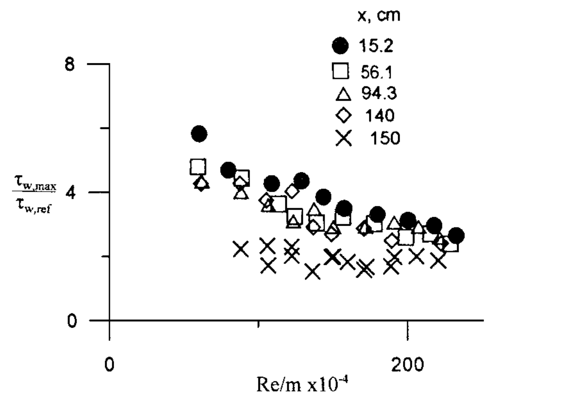

Fig. 3 Maximum surface shear stress compared to the upstream ($x = 15.2$ cm) mean value.

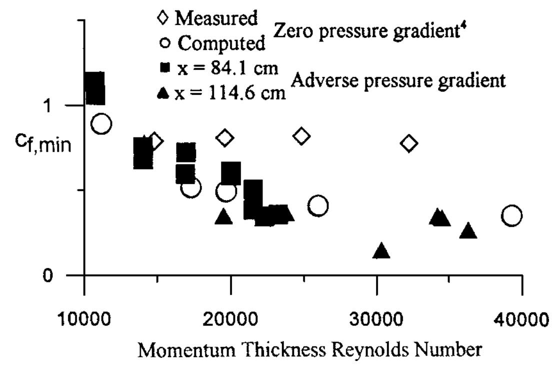

Fig. 4 Estimated minimum skin-friction coefficient.

III. Flow Model

Modeling of the individual coherent events might be expected to lead to a prediction of the mean surface shear stress. A simple impulse flow model[4] demonstrated that the mean surface shear for the lowest Reynolds numbers in zero-pressure-gradient flow was caused almost entirely by the large pulses. Although the previous studies[2,4] focused on the "vortex structure" within the events as the possible origin of the shear pulses, recent measurements suggest a different physical concept. The structured events can be viewed as moving obstructions in the flow. An in-flux into the wall region of higher energy, outer flow occurs around the obstruction (coherent event) to maintain continuity. This high-energy flow produces a moving quasi-stagnation point at the surface resulting in the pulses in surface shear stress. The strong inflow would also produce or strenghten the vortex structure observed within the coherent events.

Impulsive flow similarity solutions[5] treat the case of a body set suddenly in motion. Thus, at time zero the surface shear stress is infinite, and only the decay of the shear is predicted. It can be shown[4] that the decay of the shear obtained from the impulse flow solutions was nearly the same as that obtained from the Blasius laminar boundary-layer solution

$$c_f = \frac{t_w}{\frac{1}{2}\rho U_e^2} = \frac{0.33206}{\frac{1}{2}U_e}\left(\frac{U_e \nu}{x}\right)^{\frac{1}{2}} = \frac{0.66412}{U_e}\left(\frac{\nu}{t}\right)^{\frac{1}{2}} \quad (\text{using } x = U_e t) \qquad (1)$$

where ν is the kinematic viscosity and U_e is the velocity at the edge (of the laminar) boundary layer. Employing a characteristic velocity of the coherent event, such as 0.6 of the freestream velocity, and a time t^* characteristic of the statistical passage time of the coherent event minus the rise time of the pulse (which can be neglected at the high Reynolds numbers), a minimum value of the skin-friction coefficient was estimated,[4] (assuming the ideal case where the shear decays lasts until the next pulse occurred). The computed minimum values of $c_{f,\min}$ for the zero-pressure-gradient flow are also shown on Fig. 4. The second-order similarity impulse flow solution[5] includes a term $\phi_1 U' \sqrt{t}$ added to the $1/\sqrt{t}$ term. For an adverse pressure gradient, U' (derivative of the velocity with respect to x) is negative, and so the decay of the surface shear stress will be faster than that for zero-pressure-gradient flow.

The statistical time t^* between the large pulses have been measured for zero-, favorable-, and adverse-pressure-gradient flows.[2,4] Empirical relations to estimate t^* are listed next.

Zero pressure gradient[4]:

$$T^* \equiv U_e \sqrt{t^*/\nu} = 27 + 673 R_\theta \tag{2}$$

General pressure gradient[2]:

$$\frac{c_{f,\text{mean}}}{f(H, R_\theta)} = 0.170 + 5110(\log T^*)^{-10} \tag{3}$$

(note that the constants 0.170 and 5110 were inadvertently given as 170 and 5.110×10^{-3} in Ref. 2), where

$$f(H, R_\theta) = \mathcal{S}[1.96 \times 10^{-4} + 8.96 \times 10^{-3} H^{-4}]$$

$$\mathcal{S} = 2.67 - H + \frac{2.45 \times 10^{-5}}{R_\theta} \exp \frac{-(\ln R_\theta - 14)^2}{7.39}$$

$\mathcal{S}$ is an empirical separation criterion, which is zero when $c_{f,\text{mean}} = 0$. The relatons apply for canonical, incompressible, turbulent boundary layers. The lower limit is determined by the laminar-turbulent transition. The upper limit is not known; it appears to apply[4] for $R_\theta > 2 \times 10^5$. An empirical skin-friction relation, which also can predict $c_{f,\text{mean}}$ less than zero:

$$c_{f,\text{mean}} = \mathcal{S}(1.07 H^{-2})\left(R_\theta^{-0.77} - 0.151 R_\theta^{-1.85} + 9.9 \times 10^{-4}\right) \tag{4}$$

can be used to determine T^* in terms of the mean velocity profile parameters. Modeling of the flow over the time t^* including both the large pulses and the smaller events, such as the streamwise vorticity predicted by large eddy simulation, should lead to a prediction of $c_{f,\text{mean}}$.

IV. Conclusions

Large, time-dependent, surface-shear-stress pulses dominate the surface shear stress for low-Reynolds-number flows, which is the region where most computer modeling studies apply. At higher Reynolds numbers the time between pulses becomes progressively longer, which reduces their contribution to the mean surface shear stress.

The large pulses persist into the adverse pressure regions leading to intermittent separation. The minimum surface shear stress in the turbulent boundary layers appears to be limited by simple viscous decay. The timescale between pulses is a characteristic time related to the production of the surface shear stress in turbulent boundary layers.

References

[1] Jimenez, J., and Moser, R. D., "Large Eddy Simulation: Where Are We and What Can We Expect," *AIAA Journal*, Vol. 38, No. 4, 2000, pp. 605–661.

[2] Sandborn, V. A., "Turbulent Boundary Layer Shear Stress Pulses in Adverse Pressure Gradients," *Proceedings of the 7th AIAA/ASME Joint Thermophysics and Heat Transfer Conference*, edited by B. F. Armaly, HTD-Vol. 357-2, American Society of Mechanical Engineers, New York, 1998, pp. 95–101.

[3] Sandborn, V. A., and Kline, S. J., "Flow Models in Boundary Layer Stall Inception," *Journal of Basic Engineering*, Vol. 83, Series D, No. 3, 1961, pp. 317–327.

[4] Sandborn, V. A., "Surface Shear Stress and Heat Transfer Pulses in Turbulent Boundary Layers," *Turbulence and Shear Flow—1*, edited by S. Banerjee and J. K. Eaton, Begell House, New York, 1999, pp. 1303–1308.

[5] Watson, E. J., "Boundary Layer Growth," *Proceedings of the Royal Society of London, A*, Vol. 231, 1955, pp. 104–116.

J. C. Hermanson
Associate Editor

Influence of the Wall Condition on k–ω Turbulence Model Predictions

Frédéric Thivet,* Mirna Daouk,† and Doyle D. Knight‡
Rutgers University, Piscataway, New Jersey 08854

Introduction

As compared with other two-equation formulations, the k–ω turbulence model[1] seems easier to implement in a numerically robust manner because it does not use any damping function near the walls. However, this formal simplicity is counterbalanced by a high sensitivity of the solutions to the boundary conditions (BC) applied to solve the equations. The sensitivity of the k–ω model to the freestream values of the turbulent quantities is now a well-documented problem,[2,3] which is solved by using two-layer k–ϵ/k–ω formulations[4] for instance. With the wall condition for the turbulent kinetic energy being straightforward ($k_w = 0$), the only questionable BC is the wall condition for ω, which is theoretically infinite at a perfectly smooth wall. Wilcox[1,3] proposes to enforce the asymptotic behavior of ω ($\beta_0 \omega \sim 6\nu_w/y^2$, where $\beta_0 = 0.09$, y is the normal distance to the wall, and ν_w is the molecular viscosity at the wall) on five to seven points above the wall and under $y^+ = 2.5$ [hereafter, the superscript + denotes scaled lengths in wall units: $y^+ = y u_\tau / \nu_w$ with $u_\tau^2 = \nu_w (\partial U/\partial y)_w$ and U is the velocity in the freestream direction]. This very stringent condition, namely the smooth-wall BC for ω, is generally much too expensive to observe in three-dimensional Navier–Stokes computations, so that the alternative is usually to apply the rough-wall BC[1,3]:

$$\omega_w = N \nu_w / k_s^2 \qquad \text{with} \qquad N = 2500 \tag{1}$$

where k_s is the surface-roughness height. Physically, the flow is insensitive to the roughness height when below five wall units.[5] With such a value the rough-wall condition is expected to be hydrodynamically smooth.[1,3] It is the purpose of this Note to clarify the behavior of the flat-plate boundary-layer solutions obtained with the k–ω model in the range of the hydrodynamically smooth rough-wall BCs for ω.

Numerical Tools

Three numerical codes are used: GASP,[6] EDDYBL,[3] and CLIC2.[7] GASP solves the three-dimensional, compressible, Reynolds-averaged Navier–Stokes equations. The convective fluxes are computed to third-order accuracy using the Roe scheme and the MUSCL reconstruction method with the Min-Mod limiter. The viscous terms are evaluated by second-order central differencing. EDDYBL and CLIC2 solve the compressible, two-dimensional, laminar, transitional, and turbulent boundary-layer equations. Both codes use an adaptive technique to generate the mesh so that the solutions are always fully grid converged. GASP runs the rough-wall BC for ω, EDDYBL the smooth-wall BC, and CLIC2 can run both. In the freestream the turbulent variables are chosen in the range

Received 10 October 2000; revision received 7 July 2001; accepted for publication 8 August 2001.

*Visiting Research Scholar, Department of Mechanical and Aerospace Engineering; permanent position: Senior Research Engineer, Department of Models for Aerodynamics and Energetics, ONERA, 31055 Toulouse, Cedex 4, France. Member AIAA.

†Undergraduate Student, Department of Mechanical and Aerospace Engineering; currently Graduate Student, Department of Aeronautics and Astronautics, Massachusetts Institute of Technology, Cambridge, MA 02139.

‡Professor, Department of Mechanical and Aerospace Engineering. Associate Fellow AIAA.